High Output Maximum Efficiency Prototype Diode Pumped Laser for Space Application

Donald B. Coyle
NASA/Goddard Space Flight Center, Code 920, Greenbelt, MD 20771
barry@cornfed.gsfc.nasa.gov

Richard B. Kay, Paul R. Stysley, Demetrios Poulios
Department of Physics, American University, Washington, DC 20016

Abstract:
We report on the design and development of a prototype space-flight laser called the High Output Maximum Efficiency Resonator (HOMER). This stand-alone oscillator employs an unstable resonator cavity in a concave-convex configuration with a Gaussian graded reflectivity mirror (GRM) as an output coupler. Output energies 20 mJ at a pulse repetition frequency (PRF) of 100 Hz and 17 mJ at a PRF of 240 Hz are obtained. At 17 mJ and 240 Hz, the optical efficiency is ~16% which translates to a wall-plug efficiency ~ 7 %. The laser is conductively cooled, employs a flight-like head and optical mounts and is housed in an airtight container. It draws on the heritage of a predecessor laser of similar design which operated for > $5x10^9$ shots without damage.

OCIS codes: *280.3640, 140.3540, 140.3580, 140.5560, 140.6810, 140.3480.*

1. Oscillator Architecture

The HOMER laser shown in Figure 1. HOMER is a 2nd generation unstable resonator zig-zag side-pumped slab laser developed to achieve efficient, damage-free operation at 15-20 mJ. The design uses the minimum number of components for possible space-based remote sensing deployment. The GRM is used to achieve near-TEM_{oo} output and produce large beam sizes (0.9-1.1 mm) in a relatively small cavity length. The empty cavity design employed a geometrical length of 41 cm with an effective 33% reflective GRM with a radius of -237 cm and an HR reflector of radius +250 cm, providing a total magnification of M_t = 1.4. Magnification directly affects the dissipative losses, higher-order mode discrimination, alignment sensitivity, and the GRM spot size relative to the beam size in the active media [1-3].

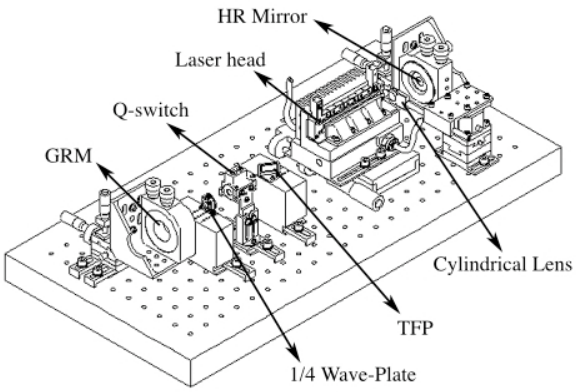

Fig. 1.The HOMER configuration. It was important to have modularity and micrometer motion control on the head and end mirrors for thorough performance characterization.

The zig-zag slab has near-Brewster end faces, a center length of ~90 mm along its optical z-axis, a thickness of 2.65 mm, (x-axis) and a 5.0 mm width (y-axis). The zig-zag slab geometry cancels optical distortion in the zig-zag plane (x-axis) to first order, and side-pumping in this plane takes advantage of the multi-stripe diode array geometry, allowing efficient pump energy coupling into the intra-slab mode volume [4,5]. We used seven 4-bar stacks of back-cooled diode arrays that are rated at 60 W/bar and collectively collimated by a single cylindrical undoped YAG lens. The slab was coated for 2-pass pumping in order to enhance the pump beam absorption. The pump diodes had ~50% electrical-to-optical efficiency upon procurement, and were typically operated at ~20% below the peak output power in order to extend their operational lifetime.

2. Laser Optimization and Compensation for Thermal Lensing

A positive thermal lens normal to the zig-zag plane (y-axis) is created in the slab as a function of average pump power and lasing efficiency. The slab lens changes strength as the laser achieves steady-state performance due to stimulated emission cooling. This effect was readily seen in the near- and far-field (FF) beam image analysis. A negative cylindrical lens (f = -65 cm) was placed next to the slab to compensate for the positive slab lens. The FF profile and cavity beam spot sizes on the HR and GRM mirrors were monitored. The HR mirror images were critical in order to track the intracavity fluence. For this laser design, a fluence of ~2.4 J/cm^2 has been measured during the performance tests discussed below.

In the predecessor laser, it was found that a fluence below 3 J/cm^2 produced reliable, damage-free operation [6]. When run above this value, small μm-size pits would develop on the slab's AR coated pump face. All the accumulated slab damage data indicates that small scale self-focusing due to longitudinal mode beating is the probable cause for slab micro burning. We have learned to precisely control these effects, and produce a very reliable transmitter without the need for single-frequency operation. The beam sizes on the HR and GRM were compared to computer resonator modeling results, which allowed us to determine the effective strength of the thermal lens under operation, and helped to fine tune the final operation of the laser for optimal beam quality, efficiency and reliability.

3. Summary of Long-term Performance Study to Date

After completing its initial configuration tests, HOMER was enclosed in its airtight container and put into a long-term performance study, which is currently continuing. Figure 2 shows the output

performance for the first 8.5×10^8 shots, as of May 9, 2005. By the time of the ESTC, the laser should have run for ~ 2×10^9 shots and that data will be presented at the conference. The energy

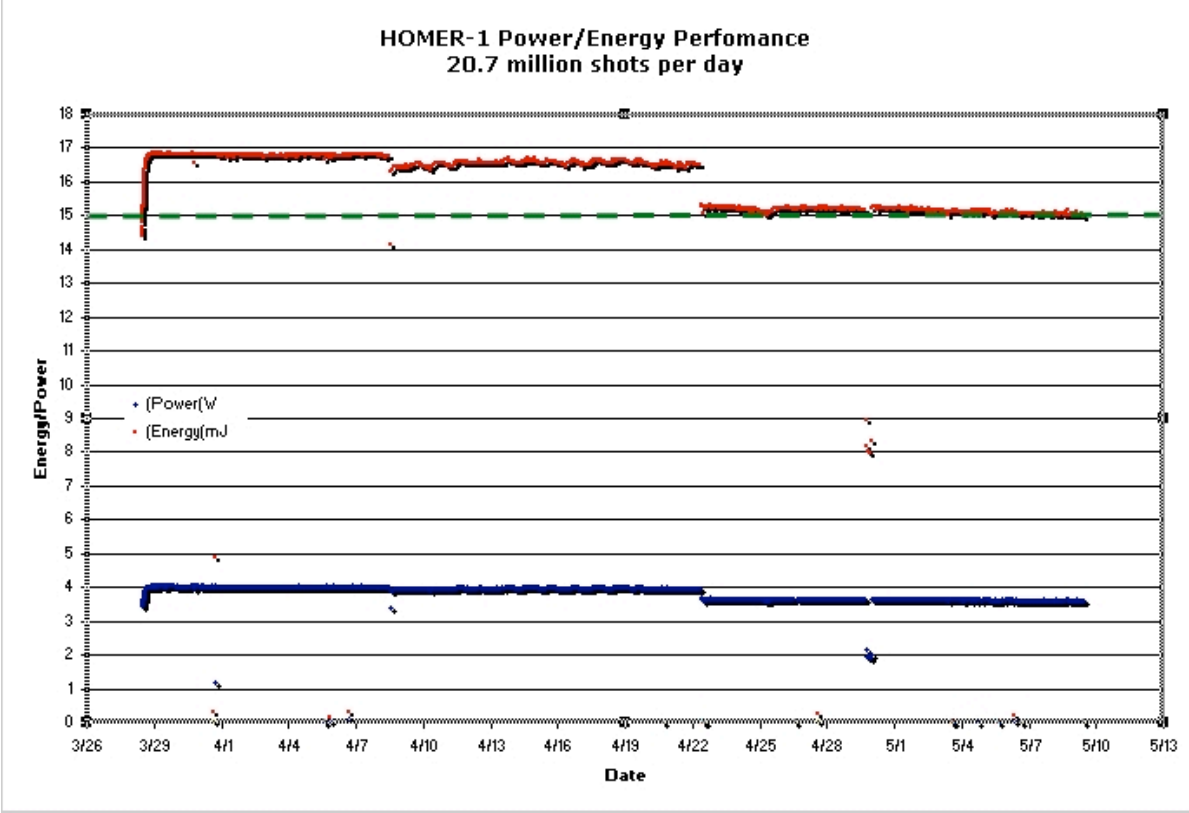

Fig. 2. Average energy and power output data for 1st 850 million shots.

loss seen on 4/22 is due to a single bar failure of one of the 28 bars making up the pump beam. This can be compensated for by increasing the diode drive current, which is running well below the specification level for these arrays. The jitter on the pulse energy plot between 4/9 and 4/22 is due a combination of a thermal heating event on 4/9, which increased the laser temp by 10°C, and a measurable seasonal change from winter to spring.

It was also important to ensure that acceptable beam quality was maintained over the test period. The typical $1/e^2$ FF divergence averaged 0.93 mR in the x-axis and 1.15 mR in the y-axis. The beam sizes on the HR averaged 1.7 mm and 2.1 mm for the x- and y-axis, respectively, before the event on 4/22/05. After that event, the beam sizes on the HR averaged 1.5 mm and 2.0 mm for the x- and y-axis, respectively. Examples of FF and HR beam images are shown in Figure 3a and 3b, respectively. The GRM and FF data provided average M^2 values of approximately M^2_x=1.48 and M^2_y= 1.53.

The optical efficiency at the beginning of the performance test was ~ 16%, which fell to ~ 15.4% after 4/22. Except for the loss of a bar, the laser output was nearly stable, decreasing by about 1% for the first 500 million shots, and continued to decrease at a similar rate after the episode on 4/22.

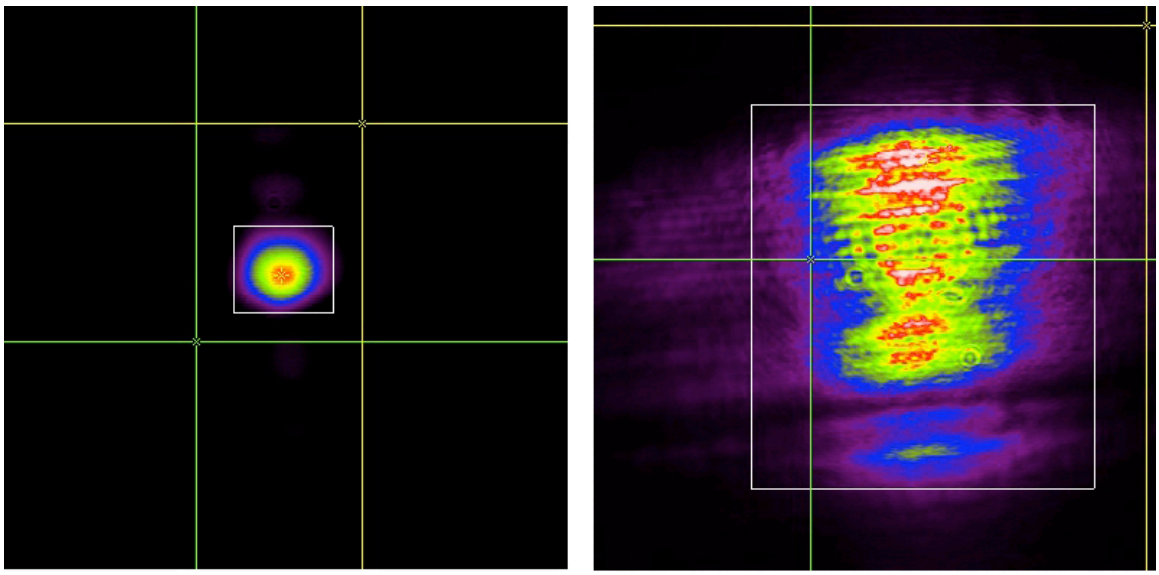

Fig. 3. (a) Typical HELT far field output pattern. (b) The HELT beam image on the HR mirror was monitored to keep track of intracavity fluences.

The HOMER laser bench and enclosure are shown in Figure 4. Note the flight-like head is thermally isolated from, and positioned near the center of, the optical bench instead. This improves mechanical and thermal stability.

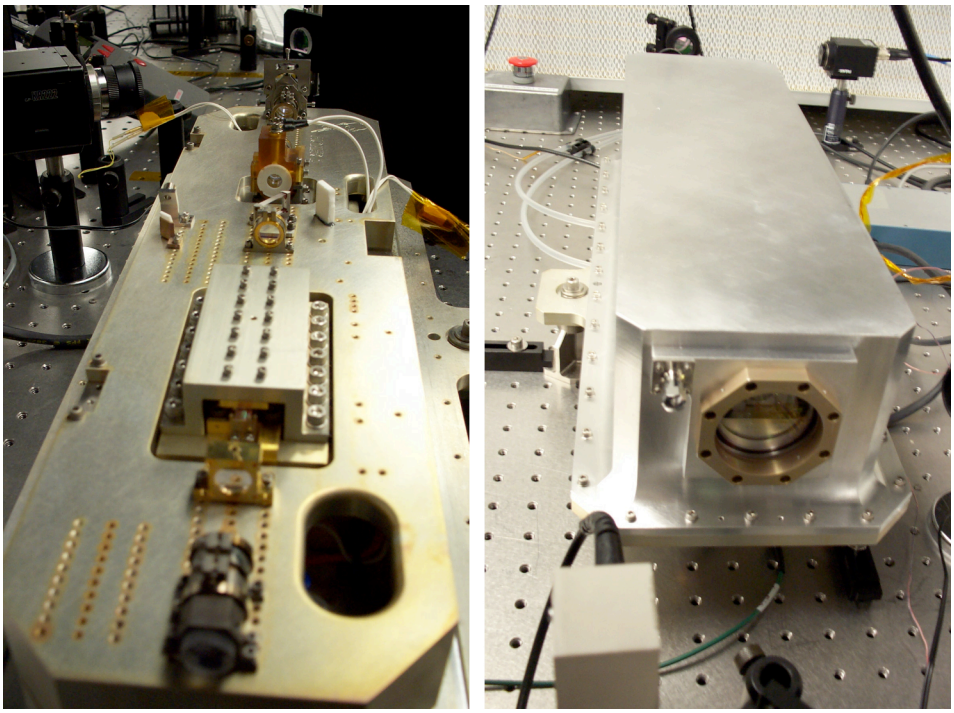

Figure 4: Laser bench is to the left and the air-tight enclosed laser on the right.

4. Conclusions

HOMER has successfully completed all preliminary tests and is in the process of a multi-billion shot operational test. The pump diodes are operating ~ 30% below design levels, The intra-cavity fluence has remained near 2.4 J/cm^2, well below the previously experimentally established limit of $\leq$ 3 J/cm^2 [7]. Continued work is planned to move the HOMER design even closer to flight readiness with planned improvements in optomechanics as well as vacuum versus pressurized studies in its airtight enclosure. A diode based 1064 nm seeder is under development and when employed with this laser would provide a significant increase in the fluence limit. The final operational range and damage limits are still to be determined, and an assessment on total system complexity, cost, and reliability is needed.

5. References

1. A. E. Siegman, "Unstable optical resonators for laser applications," Proc. IEEE **53**, 277-287 (1965). See also Sooy, IEEE JQE **5**, 575 (1969).
2. S. De Silvestri, P. Laporta, M. Magni. and O. Svelto, "Solid-State laser unstable resonators with tapered reflectivity mirrors: the super-Gaussian approach, " IEEE JQE **24**, 1172-1177 (1988).
3. M. Morin, "Graded reflectivity mirror unstable laser resonators," Opt. and QE **29**, 819-866 (1997).
4. T. J. Kane, R. C. Eckardt, and R.L. Byer, "Reduced thermal focusing and birefringence in zig-zag slab geometry crystalline lasers," IEEE JQE **19**, 1351-1354, (1983).
5. J.M. Eggleston, T.J. Kane, K. Kuhn, J. Unternahrer, and R.L. Byer, "The slab geometry laser-part I: theory," IEEE JQE **20**, 289-301 (1984).
6. D. B. Coyle, R. B. Kay, S. J. Lindauer, "Design and performance of the vegetation canopy lidar (VCL) laser transmitter," in Aerospace Conference Proceedings, (Institute of Electrical and Electronics Engineers, New York, 2002), **3,** pp: 1457 –1464.
7. D.B. Coyle, R.B. Kay, P.R. Stysley, and D. Poulios, "Efficient, Reliable, Long-Lifetime, Dioode-Pumped Nd:YAG Laser for Space-Based Vegetation Topographical Altimetry", App. Opt. **43**, 5236-5242 (2004).